applied sciences

MDPI

Article

Effect of the Front and Back Illumination on Sub-Terahertz Detection Using n-Channel Strained-Silicon MODFETs

Juan A. Delgado-Notario [1], Jaime Calvo-Gallego [1], Jesús E. Velázquez-Pérez [1], Miguel Ferrando-Bataller [2], Kristel Fobelets [3] and Yahya M. Meziani [1,*]

1 NanoLab, Universidad de Salamanca, Plaza de la Merced, Edificio Trilingüe, 37008 Salamanca, Spain; juanandn@usal.es (J.A.D.-N.); jaime.calvo@usal.es (J.C.-G.); js@usal.es (J.E.V.-P.)
2 Departament of Communications, Telecommunication Engineering School, Universitat Politecnica de Valencia, 46022 Valencia, Spain; mferrand@dcom.upv.es
3 Department of Electrical and Electronic Engineering, Imperial College London, Exhibition Road, London SW7 2BT, UK; k.fobelets@imperial.ac.uk
* Correspondence: meziani@usal.es; Tel.: +34-923-294436

Received: 31 July 2020; Accepted: 25 August 2020; Published: 28 August 2020

Abstract: Plasma waves in semiconductor gated 2-D systems can be used to efficiently detect Terahertz (THz) electromagnetic radiation. This work reports on the response of a strained-Si Modulation-doped Field-Effect Transistor (MODFET) under front and back sub-THz illumination. The response of the MODFET has been characterized using a two-tones solid-state continuous wave source at 0.15 and 0.30 THz. The DC drain-to-source voltage of 500-nm gate length transistors transducing the sub-THz radiation (photovoltaic mode) exhibited a non-resonant response in agreement with literature results. Two configurations of the illumination were investigated: (i) front side illumination in which the transistor was shined on its top side, and (ii) back illumination side where the device received the sub-THz radiation on its bottom side, i.e., on the Si substrate. Under excitation at 0.15 THz clear evidence of the coupling of terahertz radiation by the bonding wires was found, this coupling leads to a stronger response under front illumination than under back illumination. When the radiation is shifted to 0.3 THz, as a result of a lesser efficient coupling of the EM radiation through the bonding wires, the response under front illumination was considerably weakened while it was strengthened under back illumination. Electromagnetic simulations explained this behavior as the magnitude of the induced electric field in the channel of the MODFET was considerably stronger under back illumination.

Keywords: Terahertz; SiGe; MODFET; silicon; electromagnetic simulation

1. Introduction

Over the last two decades, the progress in new semiconductor materials and devices has fostered the research of room-temperature Terahertz (THz) detectors [1]. The portion of the electromagnetic (EM) spectrum located between the infrared region and the RF/microwaves one is commonly known as the Terahertz or submillimeter region and THz radiation is also referred as T-rays. The broad range of potential applications of THz radiation has fueled the research on THz sources and detectors to the point that these new devices start to be exploited in real-world applications which will be brought to market [2,3].

Accordingly, different emerging applications based on THz science developments have been investigated so far [4]. An extensive list of different fields that may potentially benefit from new THz sensing devices and techniques includes astronomy [5], spectroscopy (many chemicals can

have distinctive spectroscopic fingerprints in the THz range) [6,7], telecommunications (systems operating in the submillimeter range have a bandwidth inherently higher than those working in microwaves: for instance, THz systems will be able to meet the needs of upcoming 5–10 Gb/s data rates in point-to-point wireless short-range communications [8,9]), security screening (THz beams can be used to detect hidden objects in clothing, envelopes and materials used in packaging, additionally, some hidden substances such as plastic explosives can be detected using their Terahertz fingerprint) [10], metrology [11], etc.

At the beginning of the nineties, Dyakonov and Shur [12,13] presented a ground-breaking work that proposed and demonstrated the ability of sub-micron FETs (Field-Effect Transistors) to detect terahertz radiation. The detection was based on the nonlinear properties of the two-dimensional (2D) electron plasma in the channel of FETs. While the proposal of Dyakonov and Shur was a theoretical work, in the course of the following years the detection of sub-terahertz radiation based on plasma waves was also experimentally demonstrated using different types of FETs such as silicon MOSFETs (Metal-Oxide-Semiconductor Field-Effect Transistor) [14], strained-Si MODFETs (Modulation-Doped Field-Effect Transistor) [15], GaN FETs [16], and graphene FETs [17].

Terahertz detectors based on the properties of the 2D electron plasmas in FET channels perform direct detection of the incoming THz radiation using a frequency down-conversion technique. In direct detection, the power of THz signals impinging on the FET top-surface is converted into dc current or voltage levels via a non-linear mechanism [12,13]: for instance, in an open-drain field-effect transistor under THz light a DC voltage will set up between its source and drain contacts as a non-linear response to the THz excitation (phovoltaic mode). Dimensions and doping-profiles of short gate FETs can be designed to tailor the frequency response of the plasma channel plasma within the terahertz range. A non-linear voltage tuning of the value of this frequency can be performed through the gate-to-source bias voltage. By combining plasma-wave detectors and new continuous-wave (CW) solid-state THz sources [18], innovative THz systems will eventually be developed and brought to market, which will benefit from the well-known properties associated with solid-state sources: scalability, reliability, and compactness.

The present paper reports on the use of field-effect transistors (FETs) based on the SiGe/Si/SiGe double-heterojunction as sub-THz plasma-waves detectors. A Π-gate $Si/Si_{0.7}Ge_{0.3}$ MODFET was used as a photovoltaic mode direct detector of CW sub-THz radiation. A key advantage of plasma-waves THz detectors based on the Si/SiGe material system when compared to the ones fabricated using III-V materials, is that the first ones can be integrated on the same chip with CMOS (Complementary Metal-Oxide-Semiconductor) circuits, since both CMOS and Si/SiGe MODFETs can share the same Si wafer. And, thus, monolithic integration of a Si/SiGe THz detector and the necessary CMOS readout circuitry on a single chip may be feasible.

The paper is organized as follows: Section 2 is devoted to materials and Methods, the Si/SiGe MODFET transistor is presented and its geometry and epilayer description are detailed, finally, a description of the set up used in the THz characterization is given. Section 3 presents the experimental and simulation results of an analysis of the device response under CW excitation at 0.15 and 0.30 THz. The study focuses on the differences of the photovoltaic response when the device receives front (the one commonly used) and back THz illumination. 3D FDTD (Finite-difference time-domain) simulations are performed to explain the results obtained in measurements at 0.3 THz.

2. Device and Experimental Setup

In this section, the strained-Si MODFETs proposed as THz detectors are presented along with the techniques and the experimental setup used in measurements.

2.1. Si/SiGe MODFET

To fabricate THz detectors based on plasma oscillations high-mobility short channels FETs must be used [12,13]. The double heterojunction SiGe/Si/SiGe allows the fabrication of extremely thin layers

of strained silicon (specifically under biaxial tensile strain) sandwiched between unstrained (relaxed) SiGe layers. Figure 1 shows the vertical lay-out of the n-channel strained-Si MODFET [19].

Both the double heterojunction and the strain of the intermediate pure-silicon layer contribute synergistically to improve the performance of FET devices that are based on the Si/SiGe material system as compared to conventional MOSFETs. On the one hand, the conduction band offsets at the Si/SiGe interface provide confinement (the conduction band offset of the heterojunction $Si/Si_{0.70}Ge_{0.30}$ is about 180 meV) for electrons in the silicon layer enabling the use of this layer as the 2D channel of n-channel FET transistors by effectively blocking vertical carrier transport and, therefore, limiting the gate current of the transistor, on the other hand, biaxial tensile strain leads to high values of the electron mobility in the 2D channel. The latter is achieved by simultaneously lowering the electron conductivity mass and the electron scattering rate in the transistor channel as compared to bulk Si MOSFETs. Strain of the silicon channel modifies the six-fold degeneracy of the minimum of the conduction band of bulk silicon, under biaxial tensile strain the two valleys with their long axis perpendicular to the hetero-interface become the minimum of the conduction band and channel electrons will essentially occupy these two valleys which reduces the electron conductivity mass [20,21]. The electron scattering rate in the strained Si channel is reduced as compared to the one in conventional unstrained channels, this is achieved both through the referred lift-off of the valley degeneracy that lowers the probability of intervalley scattering for the electrons in strained-Si channel and by the doping modulation in the structure that allows to replace the intense carrier scattering by ionized impurities in the channel of MOSFETs by the less active remote impurity scattering by the dopants in the supply layer. All the above factors contribute to build up high-mobility electron plasmas in the channel of strained-Si FETs that is a key parameter to detect THz radiation.

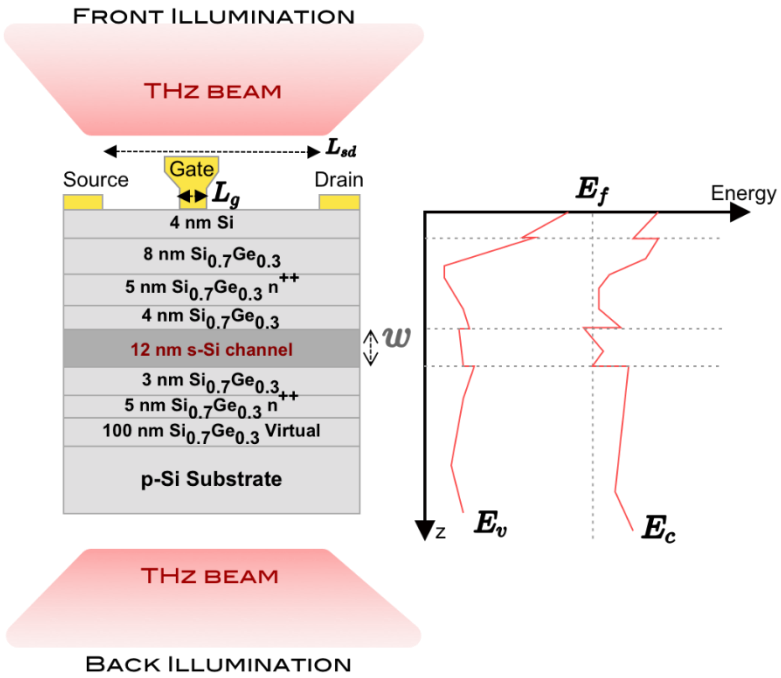

Figure 1. Left: Schematic cross section of the transistor under study. Front and back illumination configurations are highlighted by showing the respective incident THz beams in each configuration. Right: Vertical distribution of the energy band diagram under the gate at equilibrium showing the Fermi level. The double-deck supply (two unstrained n^{++} $Si_{0.7}Ge_{0.3}$ highly doped layers) sandwiching the 12 nm-thick strained silicon layer (region of thickness w highlighted in dark grey and surrounded by two nominally undoped spacer layers) generates a double quantum well inside de channel [15,19].

The fabrication of the transistor was detailed in [19]. Its horizontal layout is schematically given in Figure 1. The separation between the ohmic contacts of source and drain is L_{sd} = 2 µm. The Schottky

gate electrode had a width of 60 µm and its length (L_g) was 500 nm. Unlike in conventional FETs the gate electrode of the transistor is not equidistant from source and drain as an asymmetrical position of the Schottky-gate improves THz detection by plasma waves [19].

2.2. Terahertz Characterisation Setup

The schematic of the free-space setup used to measure the response of the transistor under sub-THz radiation is given in Figure 2. It was already described in [19]. A commercial solid-state sub-THz two-tones source was employed. The emitted power by the source at its lowest frequency (0.15 THz) was of 3 mW, while at 0.3 THz the power was 6 mW. A calibrated pyroelectric detector was used to characterize the source prior to measurements.

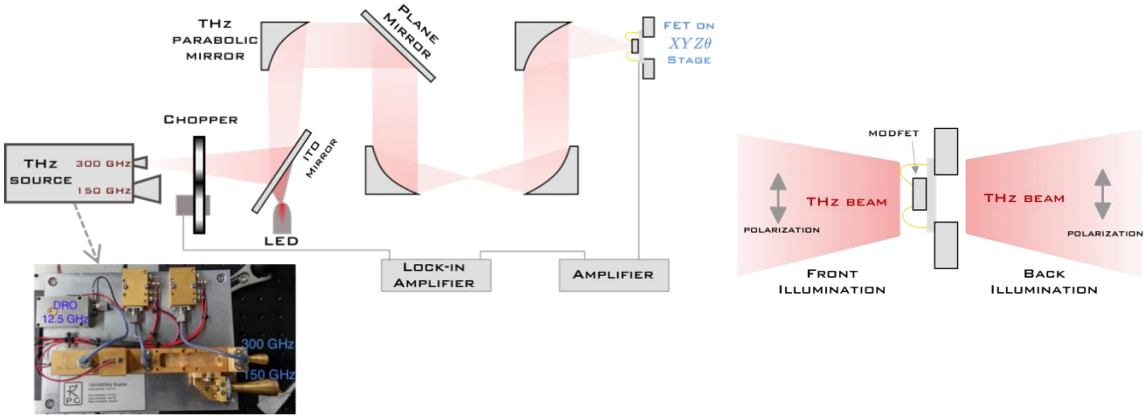

Figure 2. (**a**) Schematic description of the experimental setup: a solid-state sub-THz source by RPG (RPG-Radiometer Physics GmbH, Meckenheim, Germany) (shown in the bottom left corner) generates two output frequencies 0.15 and 0.3 THz; (**b**) Detail of the schematic of the FET detector mounted on a x-y stage with both configurations and where the THz rays polarization is highlighted.

The transistor was first wire-bounded using 25 µm-diameter pure gold wires on a DIP14 (dual in line package) as shown in Figure 3. The photovoltaic mode response of the transistor was measured using the locking technique (a Stanford Research SR830 (Stanford Research Systems, Sunnyvale, CA, USA) lock-in amplifier was used) with chopping frequency at 298 Hz. Measurements were done at room temperature.

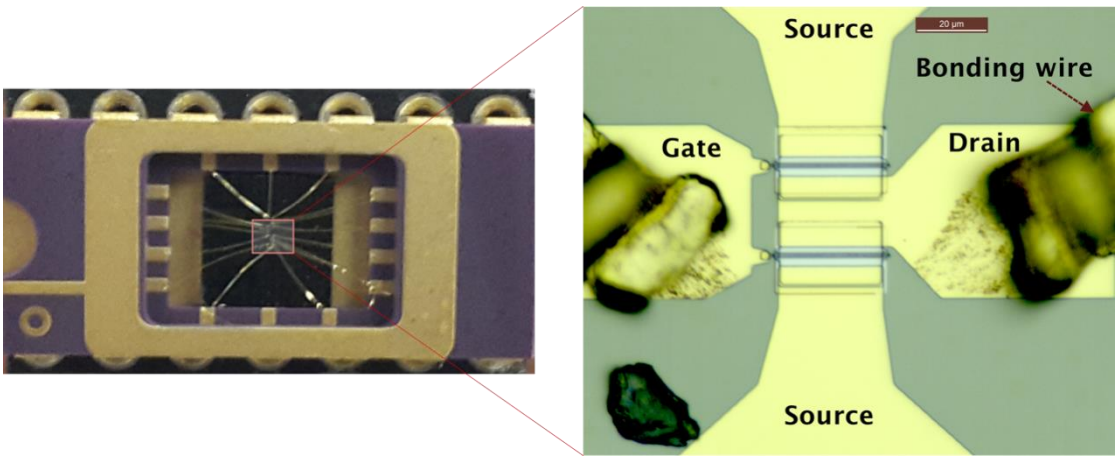

Figure 3. Left: The device under study, framed in a red rectangle for ease of viewing, glued and mounted on a DIP14 and wire-bounded to it. Right: Detailed view of the Π-gate transistor.

3. Results and Discussion

This section is essentially devoted to present and discuss an experimental study of the sub-THz response of strained-Si MODFETs under front and back illumination conditions. It is found that at 0.3 THz the response of the transistor has almost no influence of the bonding wires and, at this frequency, in contrast with the response under radiation of 0.15 THz, back illumination produces a stronger response than front illumination (the one conventionally used).

3.1. Electrical Characterization

Before wire-bonding the MODFETs were characterized on-wafer using Cascade Summit 11000B-AP probe station and an Agilent B1500A Semiconductor Device Parameter Analyzer (Agilent Technologies, Inc, Santa Clara, CA, USA). The transfer and output characteristics of the transistors are presented in Figure 4a,b, respectively. As previously reported [22,23], transistors under study are normally-on devices, i.e., a negative value of $V_{gs} < 0$ is necessary to cut-off the channel [19]. The value of the extracted threshold voltage was $V_{th} = -0.85$ V. The transfer characteristics show that when the drain voltage is moderately raised from 20 mV to 200 mV the current is greatly enhanced due to the high current throughput of the double deck electron channel. The high electron mobility in the channel induces high sensitivities of plasma waves Si/SiGe MODFETs THz sensors.

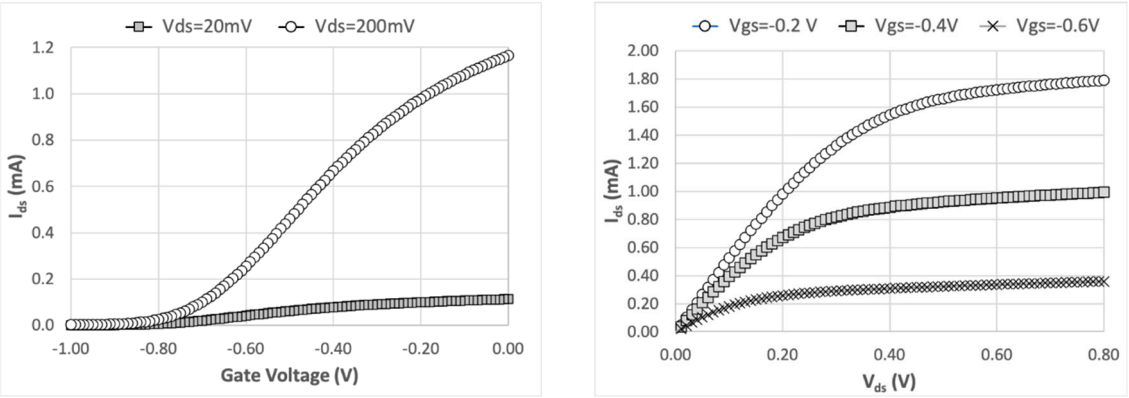

(**a**) (**b**)

Figure 4. (**a**) Transfer characteristics of the transistors under study for two values of V_{ds} (the drain-to-source voltage). (**b**) Measured output characteristics for three values of V_{gs} (the gate-to-source voltage).

3.2. Terahertz Measurements

To investigate the coupling of the incoming terahertz radiation with the channel, two types of measurements were performed: (i) front illumination where the radiation excited the device from the top side and (ii) back illumination where the transistor was excited from the bottom side (the substrate side) (see Figures 1a and 2b). It was experimentally observed that the bonding wires could play an important role to couple the incoming terahertz radiations to the channel [24,25]. This effect should be lowered if the device is excited at its back side.

Figure 5 shows the measured photoresponse under CW excitation at 0.15 THz (Figure 5a) and at 0.3 THz (Figure 5b) for both configurations: front and back illumination. The maximum of the device response in the photovoltaic mode was obtained when the gate electrode of MODFET was biased at $V_{gs} \sim -0.85$ V (i.e., the device was operating at the onset of the subthreshold region) for both frequencies and configurations setups (front and back illumination).

The detector response follows the well-known behaviour of a non-resonant (broadband) in agreement with a low value of quality factor ($Q = \omega\tau < 1$) [26] where ω is the angular frequency and τ the relaxation time. For the front illumination configuration, the photoresponse decreases by a factor of 2 (from ~400 μV to 200 μV) when the frequency rises from 0.15 THz to 0.3 THz. In contrast,

an increase by a factor of 2 is obtained under back illumination when the frequency of the source is doubled from 0.15 to 0.3 THz.

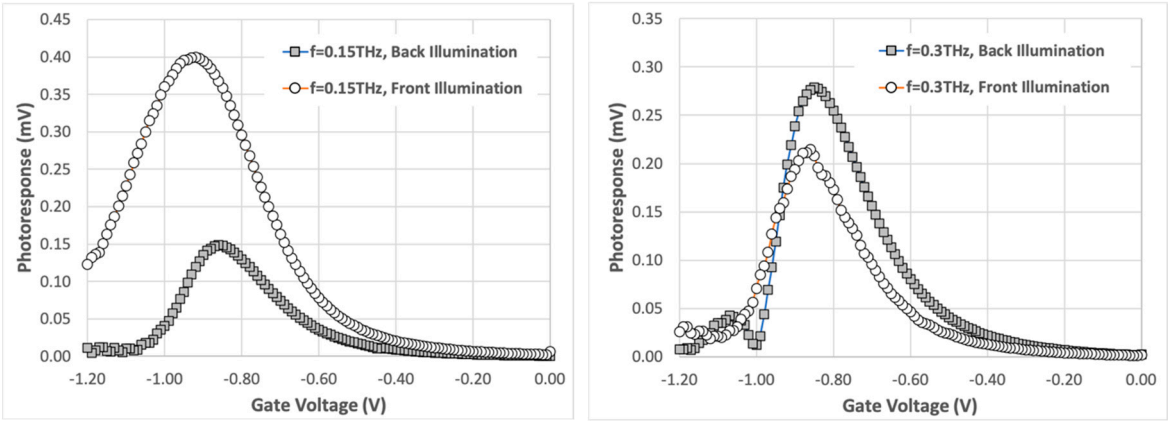

Figure 5. Photoresponse signal vs. gate voltage under excitation of (**a**) 0.15 THz and (**b**) 0.3THz and for both front and back illumination configurations.

A numerical model of the transistor was built in the electromagnetic solver software package CST^{TM} Microwave Studio. 3D simulations solving the Maxwell equations using the Time Domain Solver were performed assuming that a plane wave with a frequency of 0.3 THz propagates along the Z axis with normal incidence on the top side or on the bottom side of the transistor, i.e., front and back illumination respectively. The electric field magnitude of the incoming wave was assumed to be 1 V/m; the electric field was defined as parallel to the transistor's channel. In Figure 6 the distribution of the normalized internal electric field (E_r) induced by the impinging 0.3 THz beam along the transistor channel is given in dB as:

$$E_r(dB) = 20log_{10}\left(\frac{E}{\frac{1V}{m}}\right), \quad (1)$$

where the magnitude of the electric field in the right-hand side of equation is expressed in V/m. The magnitude of the induced electric field under back illumination (Figure 6b) is significantly higher than the one obtained under front illumination (Figure 6b) in good agreement with measurements (Figure 5b). This better coupling of the incoming power radiation to the channel is attributed to the low reflexion of the beam and transparency of the silicon substrate to THz radiation. Therefore, in silicon substrate devices, back illumination can significantly enhance the THz photoresponse of the detector. This is an interesting aspect from the technological standpoint because, as pointed out in Section 1, the silicon substrate in Si/SiGe MODFETs also provides the added advantage of CMOS compatibility.

To further investigate the above behaviour and the coupling of the terahertz radiation with the electron channel, the device was rotated in the plane perpendicular to the terahertz beam and the photoresponse signal was systematically determined for each angular position of the device. As above discussed, the maximum of the intensity of the response was obtained when the bias of MODFET gate was kept close to the value of the threshold voltage of the device for each angle.

Figure 7 gives the maximum values of the measured photoresponse signal under excitation at 0.15 THz (Figure 7a) and 0.3 THz (Figure 7b) for both configurations of the illumination (front and back). In the case of back illumination, the photoresponse signal is enhanced by a factor of two when the excitation frequency is shifted from 0.15 THz to 0.3 THz. This is mainly due to the power of the source (6 mW at 0.3 THz and 3 W at 0.15 THz). For the front illumination configuration and under excitation at 0.15 THz, four lobes were observed at ~ 30°, 120°, 190°, and 310° (blue cross marks in Figure 7a). However, for back illumination only two lobes were observed along with a lower intensity of the signal (red circles in Figure 7a). This lower intensity found in measurements under back illumination

points toward a substantial contribution of the bonding wires to the coupling of the incoming terahertz to the channel [25]. Accordingly, under excitation at 0.15 THz, the response measured under front illumination exceeds the one obtained under back illumination for any orientation of the THz beam; this can be explained as follows: for back illumination both the electron channel and the electrodes' metal pads screen the incoming EM radiation, the coupling through the bonding wires is blocked and the overall photoresponse is considerably weakened. Since the four lobes are mainly determined by the layout of the four bonding wires they are not observed in back illumination.

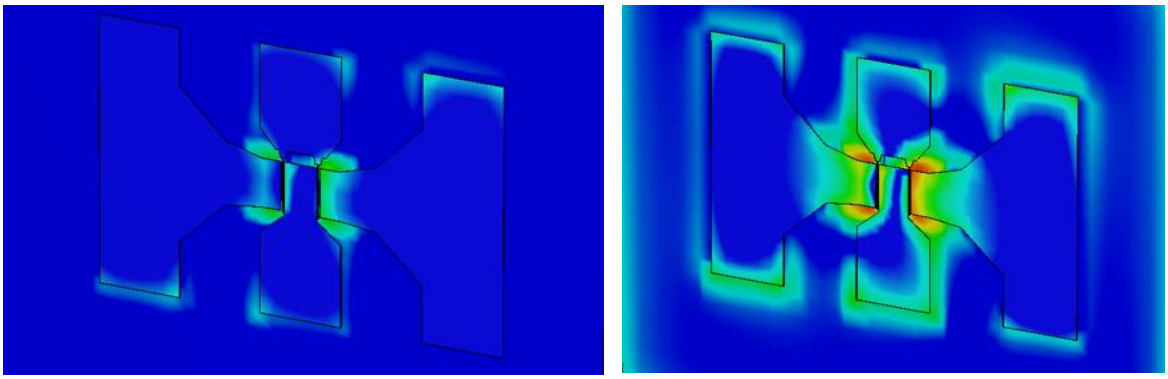

(**a**) (**b**)

Figure 6. Spatial distribution of the module of the normalized induced electric field under front, (**a**), and back, (**b**), illumination at 0.3 THz at the plane of the transistor channel (it is found in simulations that the induced electric field is mainly developed in the channel of the FET). The maximum values of the normalized electric field in the plotted plane are 18.47 dB and 29.58 dB for front and back illumination, respectively. Black solid lines indicate the contour of the top side transistor electrodes and are a guide to the eye.

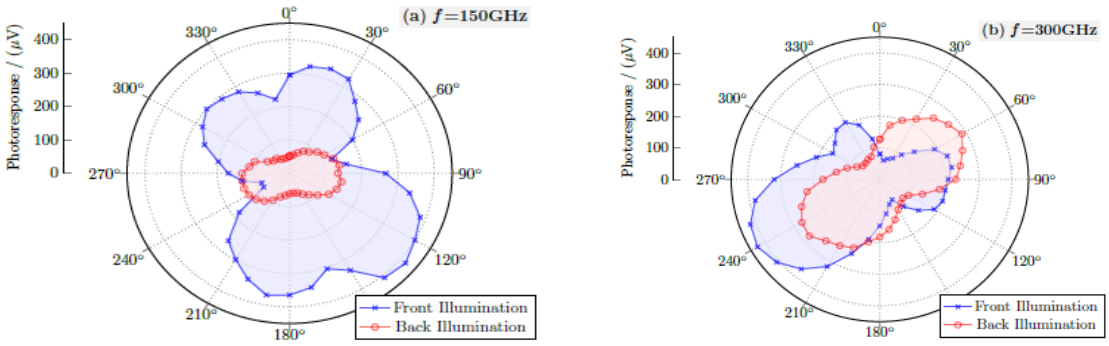

(**a**) (**b**)

Figure 7. Photoresponse signal as a function of the rotation angle under excitation of (**a**) 0.15 THz and (**b**) 0.3 THz and for both configurations front and back illumination.

For excitation at 0.3 THz measurements reveal that both device's photoresponses under both front and back illumination start to exhibit a similar dependence with respect to the THz beam orientation (Figure 7b). This is in good agreement with the weakening of the ability of the bonding wires to act as an antenna as the frequency of the THz increases [25], accordingly, since at 0.3 THz the influence of the bonding wires is lowered, both responses under front and back illumination become qualitatively similar. For the front illumination, we could observe a local maximum an important value of the measured signal for the angles around the one obtained for 330° that could be attributed to a residual coupling mediated by the bonding wires or the contacts pads. Nevertheless, this latter value is quite reduced as compared to the one observed at the angle of 240°. Moreover, a clear asymmetry of the photoresponse dependence can be observed for the angles 240° and 60° on Figure 7b under

front illumination configuration. While it is true that ideally both values should be almost equal, this asymmetric dependence could be a combined effect of a better coupling with the pads and/or the gate fingers at the angle 240° and a slight misalignment between the device mounted on the rotational axis in the plane perpendicular to the beam propagation and the THz beam during measurements.

4. Conclusions

In this work an experimental study of the response of a Π-gate Si/SiGe MODFETs (Modulation-Doped Field-Effect Transistor) under front and back sub-THz illumination was presented. The response of the strained-Si MODFET was measured using a two-tones excitation (0.15 and 0.30 THz) that were generated by a commercial solid-state continuous wave source. The DC drain-to-source voltage of the transistor transducing the sub-THz radiation (photovoltaic mode) exhibited a non-resonant response in agreement with previous results.

Two configurations of the illumination were investigated: (i) front side illumination in which the transistor was shined on its top side, and (ii) back illumination side where the device received the sub-THz radiation on its bottom side, i.e., on the Si substrate. Under excitation at 0.15 THz clear evidence of the coupling of terahertz radiation by the bonding wires was found, this coupling leads to a stronger response under front illumination than under back illumination. When the radiation is shifted to 0.3 THz, as a result of a lesser efficient coupling of the EM radiation through the bonding wires, the response under front illumination was considerably weakened while it was strengthened under back illumination. Electromagnetic simulations explained this behavior as the magnitude of the induced electric field in the channel of the MODFET was considerably stronger under back illumination.

Author Contributions: Y.M.M., K.F. and J.E.V.-P. conceived and designed the experiments; J.A.D.-N. and Y.M.M. performed the experiments; J.C.-G. and M.F.-B. performed the electromagnetic simulations; all authors analyzed the data; Y.M.M. and J.E.V.-P. wrote the original manuscript. All authors have read and agreed to the published version of the manuscript.

Funding: This research was funded by the Ministerio de Ciencia, Investigación y Universidades of Spain and FEDER (ERDF: European Regional Development Fund) under the Research Grants numbers RTI2018-097180-B-100 and TEC2016-78028-C3-3-P and FEDER/Junta de Castilla y León Research Grant number SA256P18. Also by Conselleria d'Educació, Investigació, Cultura i Esport, Generalitat Valenciana (Spain) through the grant AIC0/2019/018. The APC received no external funding.

Acknowledgments: We would like to acknowledge Thomas Hackbarth (Daimler, Stuttgart, Germany), who fabricated the strained-Si MODFETs used in this work.

Conflicts of Interest: The authors declare no conflict of interest.

References

1. Lewis, R.A. A review of terahertz detectors. *J. Phys. D* **2019**, *52*, 433001. [CrossRef]
2. Dragoman, D.; Dragoman, M. Terahertz fields and applications. *Prog. Quantum Electron.* **2004**, *28*, 1–66. [CrossRef]
3. Mittleman, D.M. Perspective: Terahertz science and technology. *J. Appl. Phys.* **2017**, *122*, 230901. [CrossRef]
4. Rainsford, T.; Mickan, S.P.; Abbott, D. T-Ray Sensing Applications: Review of Global Developments. In Proceedings of the Conference on Smart Structures, Devices, and Systems II, Sydney, Australia, 13–15 December 2004; pp. 826–838.
5. Walker, C.K. *Terahertz Astronomy*; CRC Press: Boca Ratón, FL, USA, 2015.
6. De Lucia, F. Spectroscopy in the Terahertz Spectral Region. In *Sensing with Terahertz Radiation*; Mittleman, D., Ed.; Springer: Berlin/Heidelberg, Germany, 2003; pp. 39–115.
7. Pawar, A.Y.; Sonawane, D.D.; Erande, K.B.; Derle, D.V. Terahertz technology and its applications. *Drug Invent. Today* **2013**, *5*, 157–163. [CrossRef]
8. Petrov, V.; Pyattaev, A.; Moltchanov, D.; Koucheryavy, Y. Terahertz Band Communications: Applications, Research Challenges, and Standardization Activities. In Proceedings of the 8th International Congress on Ultra Modern Telecommunications and Control Systems and Workshops (ICUMT), Lisbon, Portugal, 18–20 October 2016; pp. 183–190.

9. Federici, J.; Moeller, L. Review of terahertz and subterahertz wireless communications. *J. Appl. Phys.* **2010**, *107*, 111101. [CrossRef]
10. Federici, J.F.; Schulkin, B.; Huang, F.; Gary, D.; Barat, R.; Oliveira, F.; Zimdars, D. THz imaging and sensing for security applications—Explosives, weapons and drugs. *Semicond. Sci. Tech.* **2005**, *20*, S266–S280. [CrossRef]
11. Kleine-Ostmann, T. THz Metrology. In Proceedings of the 38th International Conference on Infrared, Millimeter, and Terahertz Waves (IRMMW-THz), Mainz, Germany, 1–6 September 2013.
12. Dyakonov, M.; Shur, M.S. Shallow water analogy for a ballistic field effect transistor: New mechanism of plasma wave generation by dc current. *Phys. Rev. Lett.* **1993**, *71*, 2465–2468. [CrossRef] [PubMed]
13. Dyakonov, M.; Shur, M.S. Mixing, and frequency multiplication of terahertz radiation by two-dimensional electronic fluid. *IEEE Trans. Electron. Dev.* **1996**, *43*, 380–387. [CrossRef]
14. Tauk, R.; Teppe, F.; Boubanga, S.; Coquillat, D.; Knap, W.; Meziani, Y.M.; Gallon, C.; Boeuf, F.; Skotnicki, T.; Fenouillet-Beranger, C.; et al. Plasma wave detection of terahertz radiation by silicon field effects transistors: Responsivity and noise equivalent power. *Appl. Phys. Lett.* **2006**, *89*, 253511. [CrossRef]
15. Rumyantsev, S.L.; Fobelets, K.; Veksler, D.; Hackbarth, T.; Shur, M.S. Strained-si modulation doped field effect transistors as detectors of terahertz and sub-terahertz radiation. *Semicond. Sci. Technol.* **2008**, *23*, 105001. [CrossRef]
16. Javadi, E.; Delgado-Notario, J.A.; Masoumi, N.; Shahabadi, M.; Velazquez-Perez, J.E.; Meziani, Y.M. Continuous Wave Terahertz Sensing Using GaN HEMTs. *Phys. Status Solidi A* **2018**, *215*, 1700607. [CrossRef]
17. Delgado-Notario, J.A.; Clericò, V.; Diez, E.; Velázquez-Pérez, J.E.; Taniguchi, T.; Watanabe, K.; Otsuji, T.; Meziani, Y.M. Asymmetric dual-grating gates graphene FET for detection of terahertz radiations. *APL Photonics* **2020**, *5*, 066102. [CrossRef]
18. Lewis, R.A. A review of terahertz sources. *J. Phys. D* **2014**, *47*, 374001. [CrossRef]
19. Delgado-Notario, J.A.; Velazquez-Perez, J.E.; Meziani, Y.M.; Fobelets, K. Sub-THz Imaging Using Non-Resonant HEMT Detectors. *Sensors* **2018**, *18*, 543. [CrossRef] [PubMed]
20. Takagi, S. Strained-Si CMOS Technology. In *Advanced Gate Stacks for High-Mobility Semiconductors*; Dimoulas, A., Gusev, E., McIntyre, P.C., Heyns, M., Eds.; Springer: Berlin, Germany, 2007; pp. 1–20.
21. Kasper, E.; Paul, D.J. *Silicon Quantum Integrated Circuits*; Springer: Berlin, Germany, 2005; pp. 207–233.
22. Gaspari, V.; Fobelets, K.; Velazquez-Perez, J.E.; Ferguson, R.; Michelakis, K.; Despotopoulos, S.; Papavassilliou, C. Effect of temperature on the transfer characteristic of a 0.5 µm-gate Si: SiGe depletion-mode n-modfet. *Appl. Surf. Sci.* **2004**, *224*, 390–393. [CrossRef]
23. Fobelets, K.; Jeamsaksiri, W.; Papavasilliou, C.; Vilches, T.; Gaspari, V.; Velazquez-Perez, J.E.; Michelakis, K.; Hackbarth, T.; Konig, U. Comparison of sub-micron Si: SiGe heterojunction nFETs to Si nMOSFET in present-day technologies. *Solid State Electron.* **2004**, *48*, 1401–1406. [CrossRef]
24. Delgado Notario, J.A.; Javadi, E.; Calvo-Gallego, J.; Diez, E.; Velazquez, J.E.; Meziani, Y.M.; Fobelets, K. Sub-micron gate length field effect transistors as broad band detectors of terahertz radiation. *Int. J. High Speed Electron. Syst.* **2016**, *25*, 1640020. [CrossRef]
25. Sakowicz, M.; Lusakowski, J.; Karpierz, K.; Grynberg, M.; Gwarek, W.; Boubanga, S.; Coquillat, D.; Knap, W.; Shchepetov, A.; Bollaert, S. A high mobility field-effect transistor as an antenna for sub-THz radiation. *AIP Conf. Proc.* **2010**, *1199*, 503–504.
26. Knap, W.; Teppe, F.; Meziani, Y.; Dyakonova, N.; Lusakowski, J.; Boeuf, F.; Skotnicki, T.; Maude, D.; Rumyantsev, S.; Shur, M.S. Plasma wave detection of sub-terahertz and terahertz radiation by silicon field-effect transistors. *Appl. Phys. Lett.* **2004**, *85*, 675–677. [CrossRef]